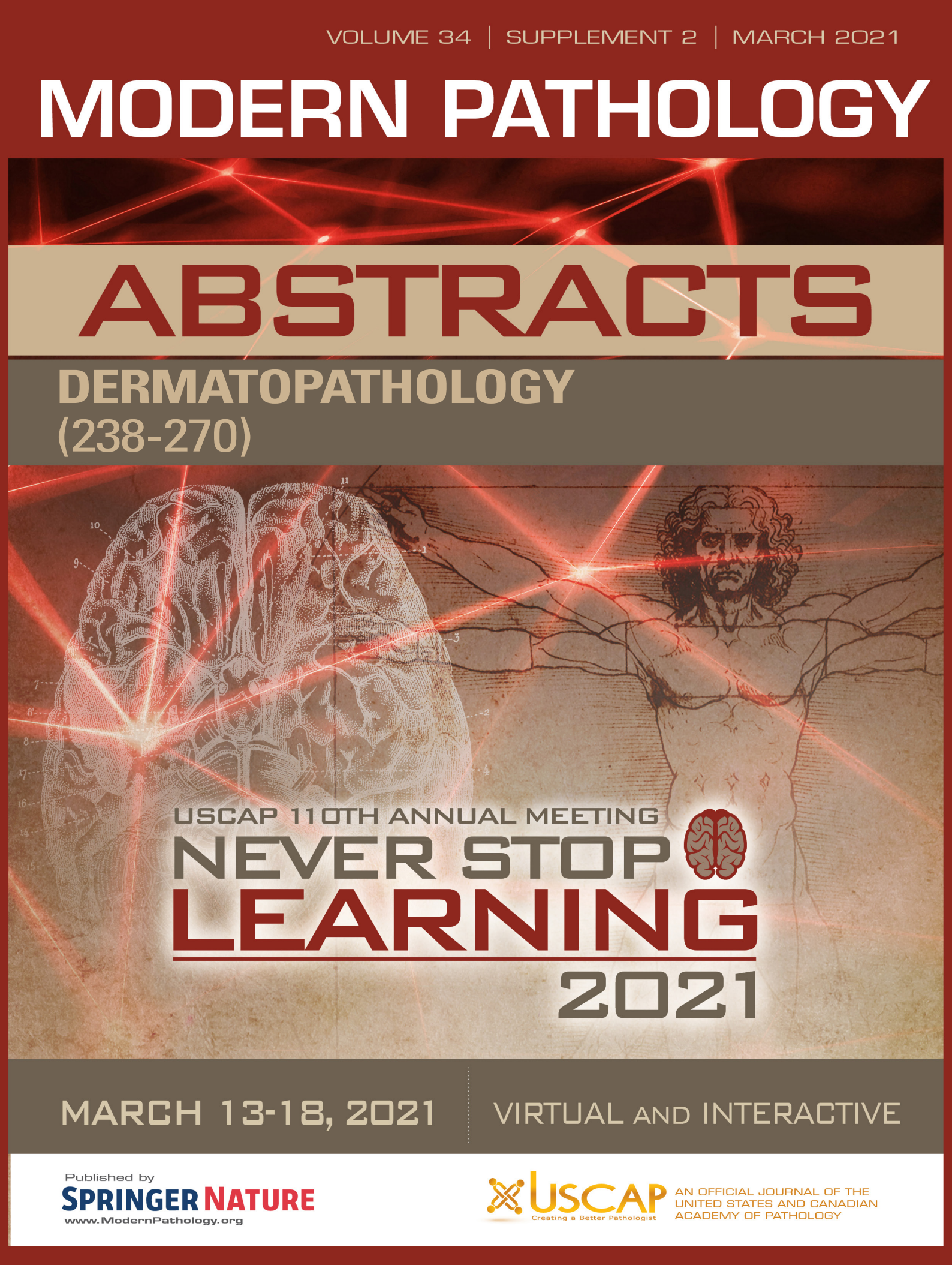


MODERN PATHOLOGY

ABSTRACTS

INFECTIOUS DISEASE PATHOLOGY
(757-770)



USCAP 110TH ANNUAL MEETING
NEVER STOP
LEARNING
2021

MARCH 13-18, 2021

VIRTUAL AND INTERACTIVE

Published by
SPRINGER NATURE
www.ModernPathology.org

 **USCAP** AN OFFICIAL JOURNAL OF THE
UNITED STATES AND CANADIAN
ACADEMY OF PATHOLOGY
Creating a Better Pathologist

EDUCATION COMMITTEE

Jason L. Hornick
Chair

Rhonda K. Yantiss, Chair
Abstract Review Board and Assignment Committee

Kristin C. Jensen
Chair, CME Subcommittee

Laura C. Collins
Interactive Microscopy Subcommittee

Raja R. Seethala
Short Course Coordinator

Ilan Weinreb
Subcommittee for Unique Live Course Offerings

David B. Kaminsky
(Ex-Officio)
Zubair W. Baloch
Daniel J. Brat
Sarah M. Dry
William C. Faquin
Yuri Fedoriw
Karen Fritchie
Jennifer B. Gordetsky
Melinda Lerwill
Anna Marie Mulligan

Liron Pantanowitz
David Papke,
Pathologist-in-Training
Carlos Parra-Herran
Rajiv M. Patel
Deepa T. Patil
Charles Matthew Quick
Lynette M. Sholl
Olga K. Weinberg
Maria Westerhoff
Nicholas A. Zoumberos,
Pathologist-in-Training

ABSTRACT REVIEW BOARD

Benjamin Adam
Rouba Ali-Fehmi
Daniela Allende
Ghassan Allo
Isabel Alvarado-Cabrero
Catalina Amador
Tatjana Antic
Roberto Barrios
Rohit Bhargava
Luiz Blanco
Jennifer Boland
Alain Borczuk
Elena Brachtel
Marilyn Bui
Eric Burks
Shelley Caltharp
Wenqing (Wendy) Cao
Barbara Centeno
Joanna Chan
Jennifer Chapman
Yunn-Yi Chen
Hui Chen
Wei Chen
Sarah Chiang
Nicole Cipriani
Beth Clark
Alejandro Contreras
Claudiu Cotta
Jennifer Cotter
Sonika Dahiya
Farbod Darvishian
Jessica Davis
Heather Dawson
Elizabeth Demicco
Katie Dennis
Anand Dighe
Suzanne Dintzis
Michelle Downes

Charles Eberhart
Andrew Evans
Julie Fanburg-Smith
Michael Feely
Dennis Firchau
Gregory Fishbein
Andrew Folpe
Larissa Furtado
Billie Fyfe-Kirschner
Giovanna Giannico
Christopher Giffith
Anthony Gill
Paula Ginter
Tamar Giorgadze
Purva Gopal
Abha Goyal
Rondell Graham
Alejandro Gru
Nilesh Gupta
Mamta Gupta
Gillian Hale
Suntrea Hammer
Malini Harigopal
Douglas Hartman
Kammi Henriksen
John Higgins
Mai Hoang
Aaron Huber
Doina Ivan
Wei Jiang
Vickie Jo
Dan Jones
Kirk Jones
Neerja Kambham
Dipti Karamchandani
Nora Katabi
Darcy Kerr
Francesca Khani

Joseph Khoury
Rebecca King
Veronica Klepeis
Christian Kunder
Steven Lagana
Keith Lai
Michael Lee
Cheng-Han Lee
Madelyn Lew
Faqian Li
Ying Li
Haiyan Liu
Xiuli Liu
Lesley Lomo
Tamara Lotan
Sebastian Lucas
Anthony Magliocco
Kruti Maniar
Brock Martin
Emily Mason
David McClintock
Anne Mills
Richard Mitchell
Neda Moatamed
Sara Monaco
Atis Muehlenbachs
Bita Naini
Dianna Ng
Tony Ng
Michiya Nishino
Scott Owens
Jacqueline Parai
Avani Pendse
Peter Pytel
Stephen Raab
Stanley Radio
Emad Rakha
Robyn Reed

Michelle Reid
Natasha Rekhman
Jordan Reynolds
Andres Roma
Lisa Rooper
Avi Rosenberg
Esther (Diana) Rossi
Souzan Sanati
Gabriel Sica
Alexa Siddon
Deepika Sirohi
Kalliopi Siziopikou
Maxwell Smith
Adrian Suarez
Sara Szabo
Julie Teruya-Feldstein
Khin Thway
Rashmi Tondon
Jose Torrealba
Gary Tozbikian
Andrew Turk
Evi Vakiani
Christopher VandenBussche
Paul VanderLaan
Hannah Wen
Sara Wobker
Kristy Wolniak
Shaofeng Yan
Huihui Ye
Yunshin Yeh
Anjana Yeldandi
Gloria Young
Lei Zhao
Minghao Zhong
Yaolin Zhou
Hongfa Zhu

To cite abstracts in this publication, please use the following format: **Author A, Author B, Author C, et al. Abstract title (abs#). In "File Title." *Modern Pathology* 2021; 34 (suppl 2): page#**

757 HPV16/18 and p16 Gene Expression in Ocular Surface Squamous Neoplasia: a Retrospective Analysis of 49 cases from Zimbabwe, Africa

Maria Carolina Beeter¹, Jonathan Lin², Yu-Tsueng Liu³, Lisa Centeno, Ahmed Ali⁴, Lovemore Gwanzura⁵, Robert Schooley³, Rangarirai Masanganise⁵

¹Stanford Health Care, Stanford, CA, ²Stanford Hospital, Stanford, CA, ³University of California, San Diego, San Diego, CA, ⁴Stanford Health Care, Palo Alto, CA, ⁵University of Zimbabwe, Harare, Zimbabwe

Disclosures: Maria Carolina Beeter: None; Jonathan Lin: None; Ahmed Ali: None

Background: Human papillomavirus (HPV) infection is an important risk factor for squamous neoplasms of the cervix, head, and neck. HPV's role in ocular surface squamous neoplasia (OSSN), including conjunctival intraepithelial neoplasia (CIN) and squamous cell carcinoma (SCC), is controversial. HIV-seropositive (HSP) populations have increased susceptibility to HPV infections, HPV-linked cancers, and markedly increased prevalence of OSSN. To determine if OSSN was related to high-risk HPV 16/18 infection in HSP patients, we performed a retrospective, cross-sectional qRT-PCR analysis of 49 OSSN patient biopsies for expression of HPV 16/18 E6/E7 viral oncogenes and the p16 tumor suppressor gene in these samples.

Design: OSSN biopsies were resected from 49 Zimbabwean patients (28 female, 21 male, ages 18-67 years), of whom 43 were HIV-seropositive (HSP). Part of each biopsy was formalin fixed, paraffin-embedded, cut, and stained with hematoxylin and eosin (H&E) to diagnose OSSN and classify as CIN or SCC. Nucleic acid was extracted from the remaining unfixed biopsy tissues and assayed by quantitative RT-PCR for p16 and HPV 16/18 E6/E7 gene transcript expression. HeLa, CaSki, and SiHa cells constitutively expressing HPV oncogenes served as positive controls. HeLa cells were also used as positive control for p16 expression, with positivity defined as p16 delta CT <10.3727 cycles. Statistical analysis of data was performed using software MedCalc v. 19. Kolmogorov-Smirnov test was performed to confirm normal distribution (parametric data). One-way ANOVA was used to compare quantitative variables. Chi-squared test was used to compare qualitative variables. The significance of the results was assessed in the form of P-value that was differentiated into non-significant when P-value > 0.05; significant when P-value ≤ 0.05; and highly significant when P-value ≤ 0.01.

Results: CIN was diagnosed in 19 of 49 OSSN biopsies (39%), and SCC in 30 of 49 biopsies (61%). Within the 43/49 HSP patients, CIN was diagnosed in 14/43 cases and SCC in 29/43 cases. All 49 OSSN cases (CIN and SCC) were negative for both HPV 16 and 18 E6/E7 oncogenes. p16 expression was detected in 13/49 OSSN cases (7 CIN cases; and 6 SCC cases). 11/13 OSSN patients that were p16+ were also HSP (5 CIN cases and 6 SCC cases); while 1/13 OSSN patient was p16+ and HIV-seronegative. 1 patient was described as HIV status "Indeterminant." No statistically significant difference was found in OSSN occurrence between men and women, chi-square test (p > 0.05). No statistically significant difference in p16 gene expression was found between subtypes of OSSNs (e.g., CIN vs SCC), analyzed by ANOVA (p > 0.05). There was insufficient power to calculate statistical significant differences between HSP and HIV-seronegative cohorts.

Conclusions: Consistent with prior studies, we found that OSSN affects men and women with no predominance in either gender. Contrary to other studies, we found no expression of high-risk HPV 16/18 E6/E7 viral gene expression in our OSSN cohort. Increased p16 gene expression was found in a minority of OSSN cases

758 Seroprevalence of SARS-CoV-2 IgG Antibodies in Health Care Workers at an Academic Medical Center in Boston, Massachusetts

Manisha Cole¹, Yachana Kataria², Elizabeth Duffy², Kyle de la Cena³, Elissa Perkins², Tara Bouton⁴, Martha Werler⁴, Cassandra Pierre², Karen Jacobson⁴, Elizabeth Ragan, Christopher Andry²

¹Boston University School of Medicine/Boston Medical Center, Boston, MA, ²Boston Medical Center, Boston, MA, ³Boston University School of Medicine, Boston, MA, ⁴Boston University, Boston, MA

Disclosures: Manisha Cole: None

Background: Severe acute respiratory syndrome coronavirus-2 (SARS-CoV-2) is a novel virus that causes Coronavirus disease 2019 (COVID-19). COVID-19 has infected over 124,813 and caused the deaths of at least 600 healthcare workers (HCWs) in the United States as of October 11th, 2020. Boston's surge was early April to mid-May, with as many as 237 COVID-19 positive patients admitted per day, a 50% rate. Seroprevalence studies are

important since the proportion of individuals that are asymptomatic with SARS-CoV-2 remains unknown and this assessment could lead to understanding disease transmission rates. HCWs are in a high-risk setting. It is important to understand disease burden among this population as it can help identify areas of high risk and inform infection control policy to slow infection rates. We aim to assess the seroprevalence of SARS-CoV-2 among HCWs at our Boston area hospital.

Design: Eligible HCWs were over 18 years old and worked on campus during the surge. With IRB approval, subjects provided consent, and completed a questionnaire regarding sociodemographic, occupation, COVID exposure, and infection prevention measures by using REDCap® database. Participants had their blood drawn between July 13th – 26th for qualitative COVID-19 IgG antibody testing. Analyses were performed by the clinical pathology laboratory, detecting IgG antibody against the SARS-CoV-2 nucleoprotein on EUA approved assay.

Results: The HCWs overall seroprevalence rate was 5.45%. Participants that were seropositive were more likely to be younger, female, and non-smokers. Obese participants had significantly higher odds of being seropositive (OR: 1.97 (95% CI: 1.25 – 3.32). Nurses (OR: 1.29 (95% CI: 0.64-3.08)) and patient facing allied health ((OR: 1.61 (95% CI: 0.74-4.22))) were more likely to be seropositive.

75.3% of participants with a positive RT-PCR test were seropositive, while 2% with a negative RT-PCR test were seropositive. 1.8% with no prior RT-PCR testing were seropositive.

Seropositivity status was significantly associated with fever, cough, shortness of breath, chills, myalgia, loss of appetite, smell and taste, and lack of physical distancing with co-workers.

Variable	SARS-CoV-2 IgG Status		p-value [†] (All Data)	RR (95% CI) (All Data)
	Positive n (row %)	Negative n (row %)		
Total	95	1648		
Sex			0.55 [†]	
Female	75 (5.8%)	1229 (94.2%)		1 (referent)
Male	20 (4.6%)	412 (95.4%)		0.79 (0.49-1.29)
Nonbinary/Third Gender	0	3 (100%)		0 (0.00-NaN**)
Age (years)			p < 0.001 ^{†*}	
<20	16 (17.2%)	77 (82.8%)		1 (referent)
20-29	17 (5.1%)	317 (94.9%)		0.28 (0.15-0.54)
30-39	22 (4.1%)	512 (95.9%)		0.23 (0.12-0.42)
40-49	15 (4.7%)	307 (95.3%)		0.26 (0.13-0.50)
50-59	20 (6.8%)	274 (93.2%)		0.38 (0.20-0.70)
60-69	5 (3.2%)	150 (96.8%)		0.18 (0.07-0.47)
>69	0	11 (100%)		0.00 (0.00-NaN**)
BMI			0.02 ^{†*}	
Underweight (<18.5 kg/m ²)	0	30 (100%)		0.00 (0.02-5.56)
Normal (18.5-24.9 kg/m ²)	39 (4.6%)	804 (95.4%)		1 (referent)
Overweight (25.0-29.9 kg/m ²)	25 (4.7%)	504 (95.3%)		1.00 (0.62-1.71)
Obese (>29.9 kg/m ²)	30 (9.0%)	305 (91.0%)		1.97 (1.25-3.32)
Hispanic/LatinX			0.05 [†]	
Yes	13 (9.1%)	130 (90.9%)		1.79 (1.02-3.14)
No	80 (5.0%)	1514 (95.0%)		1 (referent)
Race			0.54 [†]	
Asian	10 (6.3%)	150 (93.8%)		1.27 (0.66-2.42)
Black	11 (7.7%)	131 (92.3%)		1.57 (0.85-2.92)
White	63 (4.8%)	1236 (95.2%)		1 (referent)
Native American / Pacific Islander	0	7 (100%)		0.00 (0.00-NaN**)
Other	5 (4.5%)	107 (95.5%)		0.91 (0.37-2.20)
Smoking			0.33 [†]	
Yes	4 (8.5%)	43 (91.5%)		1.55 (0.59-4.04)
No	91 (5.4%)	1584 (94.6%)		1 (referent)
Occupation			0.0028 ^{†*}	
Administrative	7 (4.8%)	138 (95.2%)		1 (referent)
Allied Health – Non-Patient Facing	1 (0.9%)	111 (99.1%)		0.16 (0.02-1.31)
Allied Health – Patient Facing	19 (8.6%)	203 (91.4%)		1.56 (0.67-3.62)
Facilities Management / Support Services	0	25 (100%)		0.00 (0.00-NaN**)
Medical Doctor / Doctor of Osteopathy	18 (3.4%)	505 (96.6%)		0.63 (0.27-1.47)
Nursing	50 (7.0%)	666 (93.0%)		1.27 (0.59-2.75)

Conclusions: These results support efficacy of hand hygiene and PPE, highlighting the need to reinforce these practices when engaging with colleagues. Nurses and allied HCWs were more likely to be seropositive, likely due to frequency of exposure to positive patients or relaxed distancing among coworkers. This data suggests a higher prevalence of milder symptoms that do not always prompt caution or changes in daily activities.

759 Diagnostic Accuracy of Histochemical Stains in Identification of Mucormycetes

Nibras Fakhri¹, Gordon Love¹

¹Louisiana State University Health Sciences Center, New Orleans, LA

Disclosures: Nibras Fakhri: None; Gordon Love: None

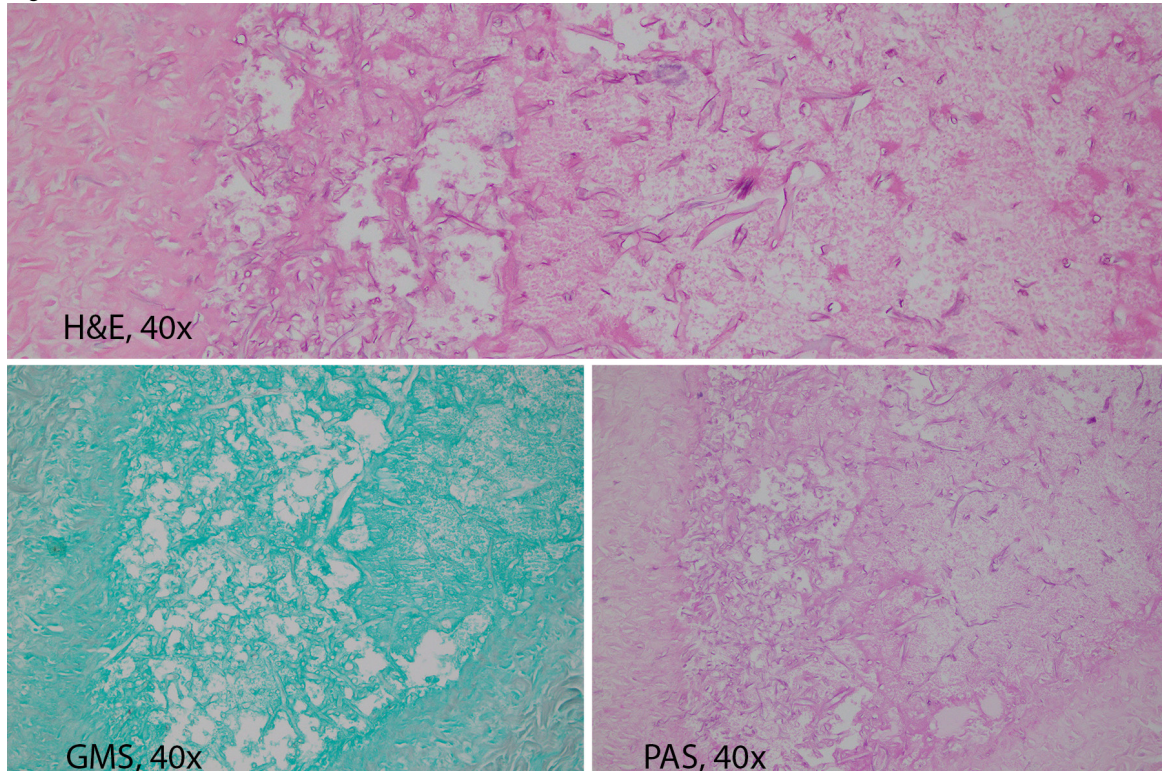
Background: Mucormycosis infection is often associated with pulmonary and disseminated disease with high mortality. Mucormycosis is a rapidly invasive disease with tissue infraction secondary to angioinvasion and fungal elements may not be readily recognizable within the resulting necrotic material. We compared the diagnostic accuracy of hematoxylin-eosin(H&E) as well as the customarily used "fungus stains"(GMS and PAS) on tissue sections from mucormycosis cases.

Design: We evaluated a total of 13 cases with invasive mucormycosis infection involving the lung, brain, spleen and the skin. Two cases are from University Medical center, New Orleans, the other 11 cases were collected from hospitals in Sacramento, California. We reviewed the histopathology of sections stained with hematoxylin-eosin(H&E), Gomori methenamine silver (GMS) and periodic acid-schiff (PAS) stains. All sections were examined carefully for fungal hyphae. We graded the intensity of GMS staining from 1+(poor), 2-3+(borderline) and 4+(strong).

Results: Histopathologically, the most prevalent feature of mucormycetes infection was the presence of abundant necrosis, angioinvasion and tissue infraction. Careful examination revealed a thin walled, slender, broad, sparsely aseptate hyphae characteristic of mucomycetes. GMS stain ranged from 1+(poor) in 6/13 cases (46.1%); 2-3+(borderline) in 2/13 (15.3%); and 4+(strong) in 5/13 (38.5%). PAS stain and H&E have the highest diagnostic performance in most cases.

Case #	Age	Sex	Site	GMS stain	Clinical history
1.	42	F	Skin, knee	4+	Right leg amputation due to truma
2.	52	F	Skin, left cheek	1+	Acute myeloid leukemia
3.	58	M	Skin	1+	Calf cyst
4.	52	F	Skin	1+	Left cheek debridement
5.	79	M	Skin	1+	Leukemia
6.	52	F	Brain	1+	IV drug abuse and hepatitis C
7.	65	M	Lung	2-3+	Fever and pulmonary consolidation
8.	34	M	Lung	1+	Empyema
9.	89	M	Bone	4+	Ethmoid bone
10.	80	M	Lung	2-3+	Acute myeloid leukemia
11.	46	M	Lung, spleen	4+	Empyema
12.	54	M	Lung	4+	Acute myeloid leukemia with pleural effusion
13.	73	M	Rhino-cerebral	4+	Diabetes mellitus and hypertension

Figure 1 - 759



Conclusions: The thin, delicate fungal hyphae embedded within the necrotic tissue and vascular lumen can be missed particularly when scanning a low magnification. Reliance upon GMS staining, the mainstay for fungal histodiagnosis, may lead to underdiagnosis of the mucormycetes. The PAS stain was better than the GMS stain that demonstrated the most limitation for staining mucormycete hyphae. PAS and H&E staining are superior for detection the mucormycetes in tissue, as early diagnosis and treatment improve patient outcome.

760 Isolated Laryngeal *Cryptococcus Neoformans* Infection in Immunocompetent Patients: Case Report and Literature Review

Karina Furlan¹, Ritu Ghai²

¹Rush University Medical Center, Chicago, IL, ²Advocate Christ Medical Center, Chicago, IL

Disclosures: Karina Furlan: None

Background: Laryngeal chronic cryptococcal infection has been increasingly described among immunocompetent individuals (1). It is acquired by inhalation of *Cryptococcus neoformans* yeasts from contaminated soil with avian excrement and generally causes a self-limited subacute pulmonary infection in immunocompetent hosts (2). Isolated laryngeal infection is rare; clinically it presents with hoarseness and is described in patients in chronic use of inhaled steroids either with COPD, asthma or with no known comorbidity (2–18).

Design: The authors present a case of isolated laryngeal cryptococcosis in a 70-year-old COPD patient and conduct a literature review in three databases: PubMed, google scholar and Scielo. The search was conducted using the following terms: “cryptococcus neoformans”, “cryptococcosis”, “larynx” and “vocal cord. Exclusion criteria were immunosuppression and/or systemic disease.

Results: The current case concerns a 70-year-old male with past medical history of COPD on chronic use of inhaled steroids who developed hoarseness refractory to oral prednisone. Direct laryngoscopy revealed an erythematous mucosa (Image 1) and a sessile mass that was excised for histological examination. Section on H&E

showed mild chronic inflammation, edema and encapsulated yeast forms highlighted by GMS and mucicarmine (Image 2).

Literature review revealed 18 peer-reviewed articles with a total of 21 patients (including the current one), M:F ratio was 9:12, median age was 69 years old, 8 patients had history of COPD and 6 had history of asthma. 20/21 patients (95%) had hoarseness as initial symptom, other symptoms included cough and laryngotracheobronchitis in one patient. 13/61 (62%) patients were chronically using inhaled steroids. The laryngoscopic findings included: white exudative patches (8, 11, 13, 14, 16, 19), erythema (9, 12), warty-like lesion (3), cystic lesion (5), sessile or polypoid lesion (12, 17, 20), “wave”-like lesion (4), asymmetry (18), thickened mucosa (14) or hyperkeratotic lesion resembling a carcinoma (6, 7). White plaques were the most common finding in 6/21 (28.5%) cases. All patients had complete resolution of the infection after variable period of oral antifungal therapy. (Table 1: compilation of all cases reported in the literature to date).

Author, date	Organism	Number of patients	Gender	Age	Comorbidity	Current medications	Location	Symptoms	Treatment	Follow-up
Reese and Colcasure 1975 (11)	<i>Cryptococcus neoformans</i>	1	Male	47	None	None	Multiple exudative lesion extending to trachea	Hoarseness	Oral fluconazole 2 months	Complete resolution in 2 months
Smallman et al, 1989(3)	<i>Cryptococcus neoformans</i>	1	Female	31	None	None	Warty lesion on the level of right vocal cord measuring 0.5 x 0.5 cm	Hoarseness	Refused	Not available
Kershner et al, 1995 (4)	<i>Cryptococcus neoformans</i>	1	Male	61	COPD, Insulin-dependent Diabetes Mellitus, 35-pack-year history of cigarette smoking, alcohol abuse	Prednisone 60 mg/day	Wave abnormality on mucosal surface	Hoarseness	6-week course of fluconazole with complete resolution of the lesion	After several months, no lesion, some hoarseness persisted
Frisch and Gnepp 1995 (12)	<i>Cryptococcus neoformans</i>	1	Male	73	Diabetes Mellitus, COPD	None	Hyperemic and fusiform mass	Hoarseness	Fluconazole 1.5 months	Symptomatic resolution after resection.
Isaacson and Frable 1996 (19)	<i>Cryptococcus neoformans</i>	1	Male	87	COPD	Inhaled steroid	Exudative white lesion on true vocal cord	Hoarseness and dry cough	Oral fluconazole 2 months	Complete resolution at 2 months
Chebbo et al, 2001 (20)	<i>Cryptococcus neoformans</i>	1	Female	66	Asthma	Inhaled and oral steroid	Laryngeal friable mass	Hoarseness	Tracheostomy, oral fluconazole	Not available
Nadrous et al 2004 (13)	<i>Cryptococcus neoformans</i>	1	Male	55	Asthma and allergic fungal sinusitis	Inhaled steroids	Leukoplakia with surrounding erythema	Hoarseness and cough	Fluconazole followed by Itraconazole	Complete resolution in 4 months
Bamba et al, 2005 (5)	<i>Cryptococcus neoformans</i>	1	Female	68	None	None	Cyst	Hoarseness	Cystectomy	No symptoms on 2-year-follow-up visit
Gordon et al, 2010 (14)	<i>Cryptococcus neoformans</i>	1	Male	64	Asthma	Inhaled steroids	Patchy leukoplakia	Hoarseness	Oral fluconazole 10 months	By the end of treatment complete resolution
		1	Female	79	None	Inhaled steroids	True vocal cord thickening	Hoarseness	Oral fluconazole 6 months	Complete resolution
Ihenachor et al, 2016 (15)	<i>Cryptococcus neoformans</i>	1	Female	82	COPD	Inhaled steroid	Diffuse ulcerative mass on false and true vocal cord, granuloma	Hoarseness and stridor	Itraconazole 6 week-course followed by Pulsed-dye laser therapy ablation and oral fluconazole 2 months	Complete resolution at month 7
Menon et al, 2016 (16)	<i>Cryptococcus neoformans</i>	1	Female	80	COPD	Inhaled steroid	Laryngeal inflammation and erythema with white patches bilaterally true vocal cords	Laryngotracheobronchitis	Fluconazole 6 months	Complete resolution on month 6
Chang et al, 2013 (17)	<i>Cryptococcus neoformans</i>	1	Male	53	Pigeon exposure	None	Posterior true vocal cord mass	Hoarseness	Fluconazole 1.5 months	Complete resolution after completion therapy
Mittal et al, 2013 (6)	<i>Cryptococcus neoformans</i>	1	Male	58	None	None	Irregular red lesion on the right vocal cord, suspicious for carcinoma	Hoarseness	Fluconazole 400 mg/daily	Complete resolution after 12 months of treatment
Tamagawa et al, 2015 (7)	<i>Cryptococcus neoformans</i>	1	Female	82	COPD, Rheumatoid arthritis	Long-term steroid treatment	Exudative, irregular region on the right arytenoid, mimicking a laryngeal carcinoma	Chronic hoarseness	Fluconazole 200 mg/daily	Complete healing after 6 months
Bergeron et al, 2015 (8)	<i>Cryptococcus neoformans</i>	1	Female	78	Asthma Atrial fibrillation Gastroesophageal reflux	Inhaled budesonide Warfarin Pantoprazole	Whitish vocal and hyperkeratosis	Chronic hoarseness	Fluconazole 200 mg twice daily ad reduction of steroid dose	Complete resolution after 4 months of treatment

Jeng et al, 2016 (10)	<i>Cryptococcus neoformans</i>	1	Female	71	COPD	Inhaled steroid	White exophytic patches on true vocal cords bilaterally	Cough and worsening of the hoarseness	KTP laser ablation and fluconazole therapy for 4 months	No recurrence of disease after 11 months.
Dangol et al, 2017 (18)	<i>Cryptococcus neoformans</i>	1	Female	83	None	Inhaled steroids	Nodular asymmetry and irregular mucosa left true vocal cord	Chronic hoarseness	Fluconazole 6 months	Improvement after 3 weeks noted
Wong et al, 2017 (9)	<i>Cryptococcus neoformans</i>	2	Female	66	Asthma and rhinosinusitis	High dose of inhaled steroid	Erythematous and thickened right true vocal cord	Chronic hoarseness	Fluconazole 200 mg twice daily and reduction of steroid dose	Complete resolution after 6 months of treatment
			Female	69	Asthma	Prednisone short course and high dose of inhaled steroid	Inflammation of the right true vocal cord	Chronic hoarseness	Fluconazole 200 mg twice daily and reduction of steroid dose	Complete resolution after 8 months of treatment
Present case	<i>Cryptococcus neoformans</i>	1	Male	70	COPD	Inhaled steroid and oral prednisone	Polypoid sessile lesion	Chronic hoarseness	Tapered off prednisone and inhaled steroid	

Figure 1 - 760

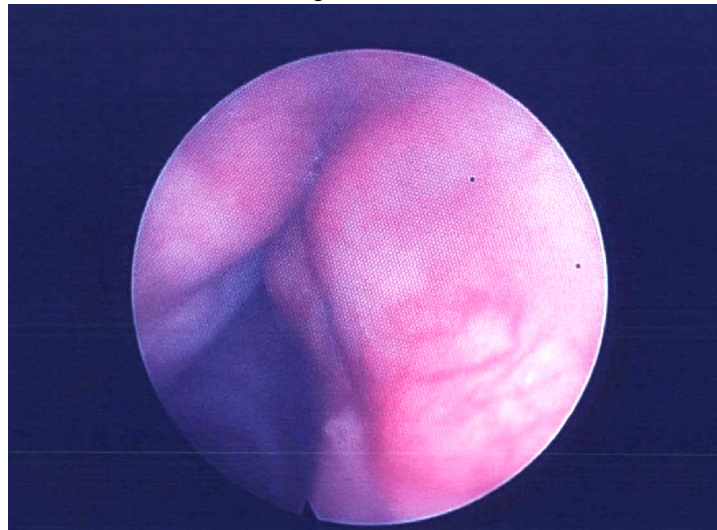
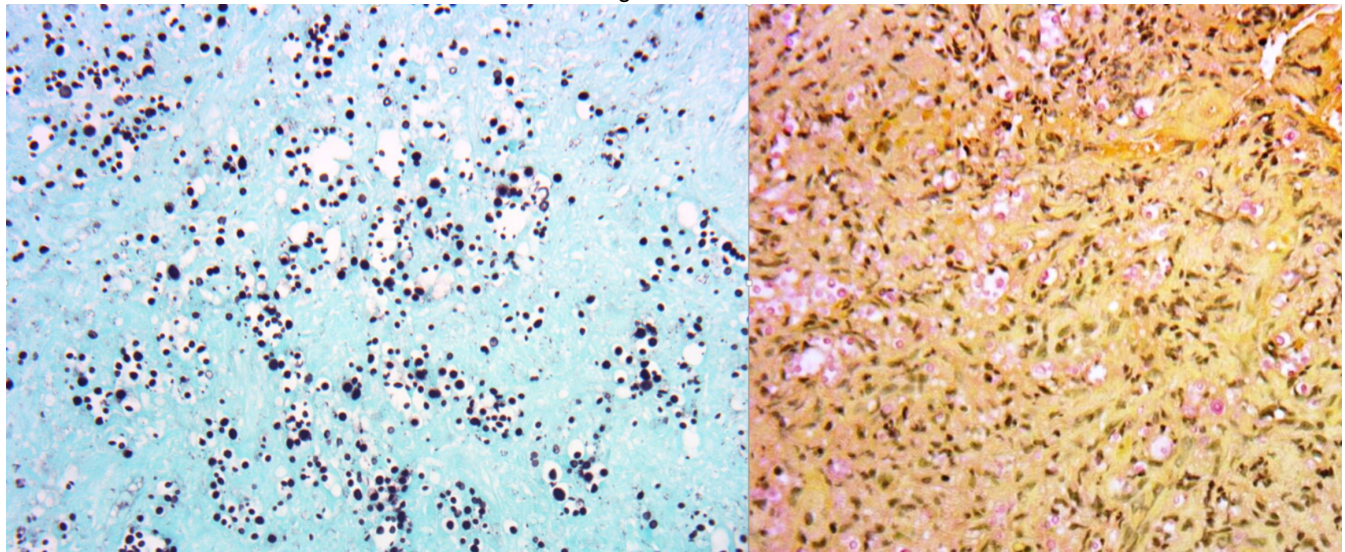


Figure 2 - 760



Conclusions: Our literature review, including the current case, revealed that isolated laryngeal infection by *Cryptococcus neoformans* shows no gender predominance, median age at diagnosis is 69 years old, patients have a past medical history of asthma or COPD in 66% of cases (14/21), white patches or plaques and erythema are the most common laryngoscopic findings (38%), 100% of patients had complete recovery after a variable period

of oral antifungal therapy. This study highlights an important differential diagnosis in immunocompetent patients who are in chronic use of inhaled steroids.

761 Evaluation of SARS-CoV-2 Nucleocapsid Immunohistochemistry as a Panfungal Screening Assay

Kara Gawelek¹, Robert Padera¹, Alvaro Laga², Isaac Solomon¹

¹Brigham and Women's Hospital, Boston, MA, ²Brigham and Women's Hospital, Harvard Medical School, Boston, MA

Disclosures: Kara Gawelek: None; Robert Padera: None; Alvaro Laga: None; Isaac Solomon: None

Background: Immunohistochemistry (IHC) is an important ancillary testing method used diagnostically and in the research setting. Our efforts to investigate the histopathologic manifestations of COVID-19 have employed a severe acute respiratory syndrome coronavirus 2 (SARS-CoV-2) IHC stain to localize virus in patient tissues. In a subset of COVID-19 autopsy cases, we observed robust off-target staining of fungal hyphae and yeast (Figure 1). While fungal elements are typically straightforward to identify in anatomic pathology specimens using H&E, Periodic acid–Schiff, or methenamine silver stains, equivocal structures are occasionally encountered, and there are no widely used fungal IHC stains. Based on these observations, we systematically investigated SARS-CoV-2 IHC staining in a wide range of fungal species to determine the generalizability and frequency of this off-target staining, and to assess for possible utility as a broad spectrum fungal staining assay to assist in cases with equivocal histochemical staining.

Design: Representative anatomic pathology cases with fungal organisms were selected, representing sixteen different fungal genera, of which 15/22 (68%) were confirmed through culture or sequencing. IHC was performed on formalin-fixed paraffin-embedded tissue sections using a rabbit polyclonal antibody derived from SARS-CoV nucleocapsid protein (NB100-56576; Novus Biologicals) with a DAB brown reaction product. In addition, off-target staining of 26 frequently utilized cell lineage and viral IHC markers was also examined in cases with *Aspergillus* sp. and *Histoplasma* sp.

Results: SARS-CoV-2 staining was present in 4/22 (18%) cases, including *Candida* spp. (n=2), *Coccidioides* sp. (n=1), and one polymicrobial case with *Fusarium* sp. IHC negative fungal elements were identified by hematoxylin counter staining in the remaining cases. Other examined IHC markers showed moderate multifocal positivity for CK7 and CEA in *Aspergillus* sp., and claudin-4 in *Candida* sp., while the 23 other markers were negative for both species.

Figure 1 - 761

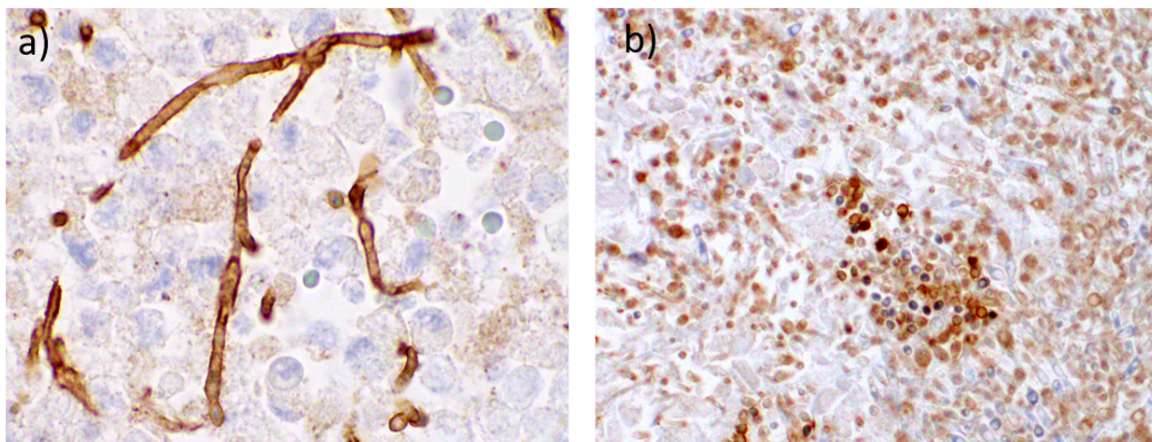


Figure 1. SARS-CoV-2 IHC highlighting a) fungal hyphae present as post-mortem colonization in a COVID-19 autopsy case and b) yeast forms in a non-COVID-19 surgical case.

Conclusions: SARS-CoV-2 IHC staining should be carefully reviewed in cases of unconfirmed COVID-19 to avoid mis-diagnosis of fungus as sloughed virally infected epithelial cells. Although fungus may occasionally stain with SARS-CoV-2 IHC or the other commonly used IHC markers tested in this study, this phenomenon is inconsistent, limiting the utility for any of these antibodies to serve as broad spectrum fungal markers.

762 Temporary Androgen Deprivation As a Simple Effective Treatment for Men with COVID-19: Preclinical Evidence

RongRong Huang¹, Andrew Goldstein¹, Liying Zhang², Takao Hashimoto³, Matthew Rettig³, Weibo Yu², Jianyu Rao², Huihui Ye²

¹David Geffen School of Medicine at UCLA, Los Angeles, CA, ²University of California, Los Angeles, Los Angeles, CA, ³UCLA Medical Center and David Geffen School of Medicine, Los Angeles, CA

Disclosures: RongRong Huang: None; Andrew Goldstein: None; Liying Zhang: *Stock Ownership*, Shanghai Genome Center; *Employee*, Shanghai Genome Center; Takao Hashimoto: None; Matthew Rettig: *Speaker*, Bayer; *Speaker*, Janssen; *Consultant*, Amgen; *Consultant*, Ambryx; *Grant or Research Support*, Novartis; Weibo Yu: None; Jianyu Rao: None; Huihui Ye: None

Background: The morbidity and mortality of COVID19 in men are reported higher than women. The entry of SARS-CoV-2 virus into host cells is mediated by the interaction between viral spike (S) protein and two host cell surface molecules: receptor ACE2 and primer TMPRSS2. Furin, another protease, may also be involved in S protein priming. TMPRSS2 is known to be transcriptionally upregulated by androgen in prostate cancer (PCa). A study from Italy showed that PCa patients on Androgen Deprivation Therapy (ADT) had a significantly lower COVID-19 incidence compared to PCa patients not on ADT. Based on those evidence, a phase II randomized multi-institutional "HITCH" clinical trial, using degarelix to rapidly suppress androgen, is currently open for hospitalized male COVID-19 patients. In this study, we aim to assess the role of androgen in regulating TMPRSS2, ACE2, and furin in respiratory epithelium, and to establish correlative tissue biomarker assays for the HITCH trial.

Design: Immunohistochemistries (IHC) for AR, TMPRSS2, ACE2, and furin were performed on tissue sections of normal human and murine upper and lower respiratory tract tissue. IHC was also performed on cell blocks prepared from nasopharyngeal (NP) swabs of 12 virus-negative individuals and 4 HITCH trial patients. Male mice were surgically castrated (N=6, all young mice) or treated with ADT drug enzalutamide (N=6, 3 young and 3 old each). Treated mice and paired untreated control mice were sacrificed. Respiratory tract and prostate tissue were harvested for IHC evaluation and western blot.

Results: Co-expression of AR, TMPRSS2, ACE2, and furin were detected by IHC in male human and murine respiratory epithelium, mainly in sinonasal, bronchial, and bronchiolar mucosa (Figure 1). AR shows weak expression in the respiratory epithelium and moderate expression in salivary glands and lacrimal glands. In females, respiratory epithelium is negative for AR and is positive for TMPRSS2, ACE2, and furin. Expression of AR, TMPRSS2, ACE2, and furin were also detected in respiratory epithelial cells prepared from NP swab specimens. In mice, castration was consistently associated with a marked reduction of AR and TMPRSS2 expression in lacrimal and salivary glands, and a moderate reduction of AR and TMPRSS2 expression in sinonasal epithelium (Figure 2). Reduction of ACE2 and furin was also observed in sinonasal epithelium after castration. Enzalutamide treatment was associated with a mild reduction in ACE2, TMRPSS2, and furin expression in sinonasal epithelium.

Figure 1 - 762

Fig 1. Co-expression of AR (blue chromogen) and TMPRSS2 (red chromogen) in human respiratory epithelium (A. Nasosinus; B. Bronchiole)

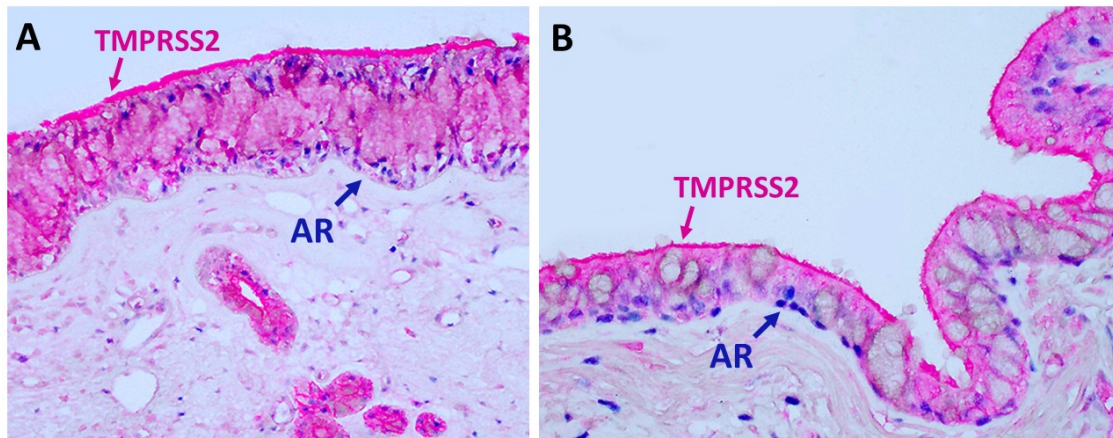
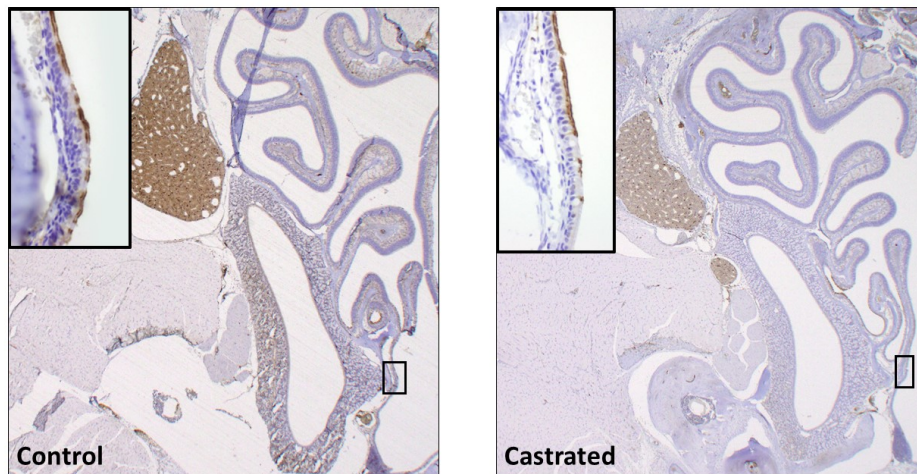


Figure 2 - 762

Fig 2. TMPRSS2 expression in nasal sinus in control and castrated mouse



Conclusions: Androgen upregulates expression of TMPRSS2, ACE2, and furin in upper respiratory epithelium in men. Our results provided preclinical evidence to explore the utility of ADT in treating men with COVID-19. The effectiveness of ADT in treating male COVID-19 patients will be tested in the HITCH trial and the biomarker correlates study.

763 Recovery from COVID19 is Associated With An Increase In CD3+, CD4+ and CD8+ T-cells During The Course of Disease

Shafinaz Hussein¹, Matthew Croken², Siraj El Jamal², Pallavi Khattar², Francine Dembitzer²
¹Mount Sinai Hospital, New York, NY, ²Icahn School of Medicine at Mount Sinai, New York, NY

Disclosures: Shafinaz Hussein: None; Matthew Croken: None; Siraj El Jamal: None; Pallavi Khattar: None; Francine Dembitzer: None

Background: The COVID19 pandemic is caused by the novel coronavirus, SARS-CoV-2 (SARS). The majority of individuals with COVID19 are asymptomatic or experience mild disease, however, a subset of patients develop serious respiratory illness. Lymphopenia, primarily affecting T-cells, is a characteristic hematologic finding associated with severe disease. Here, we characterize the changes in T-, B-, and NK-cell subsets during the disease course to determine if any have predictive value.

Design: The pathology database was utilized to identify hospitalized patients >18 years of age with SARS infection determined by PCR testing of nasal swab. Peripheral blood samples were analyzed for T-, B- and NK-cell subsets using Beckman Coulter AQUIOS Flow Cytometry System. The antibody panels were CD45/CD4/CD8/CD3 and CD45/CD16+56/CD19/CD3. Lymphocyte subset analyses were performed every 2-5 days until SARS PCR negativity, hospital discharge, or death. Disease severity was defined as follows: mild disease: SpO2>94% AND no pneumonia on imaging; moderate disease: SpO2<94% OR pneumonia on imaging; severe disease: high flow nasal cannula, non-rebreather mask, BIPAP or mechanical ventilation support. Complete blood counts with differential, IL6 and IL8 levels, and ABO/Rh blood type were recorded. Linear regression analysis was performed for each laboratory metric.

Results: 33 hospitalized patients (17 males, 16 females, age range 34-93 years, median 68 years) were included in the study. 7 patients were asymptomatic or had mild disease, 13 had moderate disease, and 13 had severe disease. 24 patients recovered, and 9 patients died. There were no readmissions for COVID19. The median absolute CD3 level ranged from 496-1509 count/uL in asymptomatic/mild patients; 291-1284 count/uL in patients with moderate disease and 67-816 count/uL in patients with severe disease. Patients who recovered had an increase in absolute CD3+, CD4+, and CD8+ counts during the course of hospitalization. Absolute B- and NK-cells trended upwards in both survivors and non-survivors, with no difference in median slope in either group. There was a downward trend in IL6 and IL8 levels in surviving patients.

Disease status	Male:female; age range	Blood type	Median absolute CD3 range counts/uL	Median absolute CD4 range counts/uL	Median absolute CD8 range counts /uL	Median absolute B cell range counts/uL	Median absolute NK cell range counts/uL
Mild/asymptomatic N=7	2M:5F; 34-89 years	5 O-type 2 A-type 6 Rh+	496.5-1509	312-804	166.5-692	66.5-321.5	109-404.5
Moderate, n=13	5M:8F; 39-93 years	6 O-type 3 B-type 2 A-type 1 AB-type 9 Rh+	291-1284.5	64-1041.5	102.5-424.5	2-1254	28.5-307.5
Severe, n=13	10M:3F; 38-83 years	5 O-type 4 B-type 4 A-type 13 Rh+	67-816.5	51-514	15-366	0-494.5	23-310

Conclusions: Recovery from COVID19 is associated with an increase in absolute CD3+ T-cells. Both CD4+ and CD8+ T-cell subsets increased over time in survivors. Lymphocyte subset analysis and increasing CD3/CD4/CD8 T-cells during disease course may be useful predictors in COVID19 infection.

764 Quality Control Practice for SARS-CoV-2 PCR Acid Detection: An Additional Quality Control MeasureLester Layfield¹, Douglas Miller¹, Simone Camp¹, Kelly Bowers¹¹University of Missouri, Columbia, MO**Disclosures:** Lester Layfield: None; Douglas Miller: None

Background: Testing for SARS-CoV-2 RNA is recommended for those symptomatic from/or exposed to the virus. Most laboratories use polymerase chain reaction (PCR) assays. Published recommendations for quality control (QC) measures mostly rely on use of known positive and negative controls which ensure the adequacy of the extraction and PCR steps but do not measure other components of testing such as specimen contamination, technologist performance or other methodologic issues.

Design: Following our laboratory's detection of a small number of false positive COVID-19 PCR tests in asymptomatic individuals, all samples from asymptomatic unexposed persons with SARS-CoV-2 positive tests were retested to confirm the initial result. When the second test was negative a third test was performed and a root-cause analysis of the error performed. RNA extraction and PCR were performed using the Thermo Fisher (Waltham, MA) or Siemens (Munich, Germany) systems.

Results: Approximately 21,000 COVID tests were performed in an 8-week period. During this period, 6,782 specimens were from asymptomatic persons of which 155 were positive. Replicate testing revealed 30 (19%) of these positive tests to be false positive results. Review of cycle threshold curves, locations of specimens on test plates and technologists' records revealed contamination and false positive sample located near a sample with a high viral load were the most common causes of erroneous results.

Conclusions: Use of only known positive and negative samples appears insufficient for adequate quality control. Focused retesting appears to be a better metric to detect contamination, carry over and technologist error. We have begun a QC program in which all positive samples from asymptomatic unexposed persons, positive samples near high viral load specimens, and 1% of negative samples from exposed symptomatic patients are retested to monitor quality of technologist performance and validity of test results.

765 The Diagnostic and Prognostic Roles of EBER for Patients With HIV-Associated Aggressive Non-Hodgkin Lymphomas In The Era of HAARTBrenda Mai¹, Wei Wang², Wen Shuai², Xiaohong Iris Wang³, Lei Chen⁴, Hilary Y Ma², Md Amer Wahed¹, Shimin Hu², Nghia Nguyen¹, Zhihong Hu¹¹The University of Texas Health Science Center at Houston, Houston, TX, ²The University of Texas MD Anderson Cancer Center, Houston, TX, ³The University of Texas Health Science Center at Houston McGovern Medical School, Houston, TX, ⁴The University of Texas at Houston, Houston, TX**Disclosures:** Brenda Mai: None; Wei Wang: None; Wen Shuai: None; Xiaohong Iris Wang: None; Lei Chen: None; Hilary Y Ma: None; Md Amer Wahed: None; Shimin Hu: None; Nghia Nguyen: None; Zhihong Hu: None

Background: HIV infection remains an increased risk to develop lymphomas in the era of HAART therapy. HIV-associated NHLs are predominantly aggressive large B cell lymphomas with a high incidence of concurrent EBV infection. However, the prognostic role of EBV infection is not well defined in this group of patients.

Design: We retrospectively reviewed the HIV+ patients with aggressive non-Hodgkin lymphomas during the interval of 2008-2019 at our institution. One subset of cases were re-classified following the 2017 revised World Health Organization criteria. Patient's clinical information and prognosis were analyzed.

Results: Our current study includes 101 patients with HIV-associated NHLs in the recent 12 years, composed of 14 women and 87 men with a median age of 45 years (range, 20-67) at the diagnosis of lymphoma. In the era of HAART therapy, EBER was positive in 34/67 cases examined and EBV-LMP1 in 5/16 cases, with ½ EBV-LMP1 positive in EBER+. Diffuse large B cell lymphomas (DLBCL) remained the most frequent type of aggressive NHLs, in 44 (44%) patients, with EBER positive in 7/19 (37%) and EBV-LMP1 3/9 (33%) cases. Plasmablastic lymphoma

(PBL) was the second most frequent, in 22 (22%) NHL patients, with EBER positive in 20/20 (100%) and EBV-LMP in 1/3 (33%) cases examined. Eighteen patients had high grade B cell lymphomas (HGBCL) with 15 NOS and 3 MYC/BCL6 rearrangements; EBER positive in 3/7 cases examined. 10 (10%) patients had diagnosis of Burkitt lymphoma (BL), with EBER positive in 2/4 and EBV-LMP1 1/3 (33%) cases. 5 (5%) patients had diagnosis of primary effusion lymphoma (PEL) with HHV8 positive in 5/5 (100%) and EBER positive in 2/3 (67%) cases. 3/5 (60%) PEL patients had preceding/concurrent Kaposi's sarcoma. Two patients (2%) were diagnosed with B-acute lymphoblastic leukemia (B-ALL), none of them were positive for EBER. With a median follow up of 10 months (range, <1.0 – 119.6), patients with NHLs had a median OS of 65 months. Patients with EBV+ NHLs had no different survival than EBV- NHLs ($p=0.86$). However, patients with EBV+ HGBCL had an inferior survival from EBV-negative HGBCL ($p=0.02$).

Conclusions: EBV infection is high in patients with HIV-associated NHLs. The utilization of EBER are not only a diagnostic marker for plasmablastic lymphoma and primary effusion lymphoma, but also a prognostic marker for high grade B cell lymphoma. We would suggest the utilization of EBER in the diagnosis and prognostic evaluation for aggressive HIV-associated NHLs.

766 Histologic, Direct Immunofluorescence, and ISH Findings in a Case Series of 3 Living COVID-19 Patients and Evidence of Prolonged Persistent Viral Replication

Romana Mayer¹, Allen Burke², Cheng-Ying Ho¹, Guanghua Wang³, Jennifer Holler⁴, Shimin Zhang⁵
¹University of Maryland Medical Center, Baltimore, MD, ²University of Maryland Medical School of Medicine, Baltimore, MD, ³The Joint Pathology Center, Bethesda, MD, ⁴University of Maryland School of Medicine, Baltimore, MD, ⁵The Joint Pathology Center, Silver Spring, MD

Disclosures: Romana Mayer: None; Allen Burke: None; Cheng-Ying Ho: None; Guanghua Wang: None; Jennifer Holler: None; Shimin Zhang: None

Background: Previously reported histopathologic and tissue viral studies have been performed on autopsy samples. Little is known about the progression of COVID-19 pneumonia within living patients and how histology, viral presence, and viral replication are affected as the disease advances.

Design: Patients who had COVID-19 positive pneumonia and underwent lung biopsies from March through June 2020 were selected for a total of 3 patients. Biopsies were taken 1 day, 19 days, and 37 days after initial COVID positive diagnosis between the 3 patients. Direct immunofluorescence (DIF) probes (GeneTex) against the SARS-CoV-2 RNA spike protein (S2 subunit) and RNA in-situ hybridization (RNAscope) probes (SARS-CoV-2 viral spike gene negative strand probe to detect viral genomic RNA and positive strand spike gene probe to detect minus-strand viral RNA for viral replication status) were applied to paraffin sections. RNAscope assay was validated comparing known positive cases with semiquantitative Real-time RT PCR for SARS-CoV-2 viral RNA.

Results: The short duration (1 day) biopsy showed mild diffuse interstitial inflammation with uniform reactive pneumocyte hyperplasia without hyaline membranes. The long duration biopsies (19 and 37 days) showed intense interstitial macrophage infiltrates; one of these had concomitant herpes simplex necrotizing pneumonitis superinfection. There were areas of organizing alveolar injury (loose fibrosis) in the 37 day biopsy. Immunofluorescence for SARS-CoV-2 protein was positive in all 3 biopsies in a pneumocyte distribution in scattered foci. Percent positive tissue inversely related to the time from initial diagnosis. RNAscope for both positive and negative strand probes was positive very focally in interstitial cells and cells in the airspaces, in the 37 day biopsy, indicating active viral replication, but negative in the others. A COVID-19 DAD control with diffuse alveolar damage (DAD) showed the greatest positivity with DIF with nearly diffuse pneumocyte staining and was focally positive in RNAscope assay (positive strand viral RNA).

Patient	Interval between onset of symptoms to biopsy	Histologic findings	Clinical Outcome	DIF (% area positive*)	ISH + Strand	ISH - Strand
37 yo F	1 day	Sparse interstitial inflammation with diffuse pneumocyte reactivity	recovery	60%	-	-
43 yo F	19 days	Interstitial mononuclear cell inflammation with patchy alveolar injury	Died one week after biopsy	50%	-	-
37 yo M	37 days	Interstitial mononuclear cell inflammation with patchy alveolar injury; concomitant focal HSV necrotizing pneumonitis	Died two weeks after biopsy	30%	+	+
Positive control	Unknown	COVID-19 Diffuse alveolar damage with hyaline membranes	Medical examiner's autopsy	100%	+	-
Negative control	N/A	Normal lung except for areas of aspiration pneumonia, COVID-19 + patient died of perforated bowel	Medical examiner's autopsy	0	-	-

Figure 1 - 766

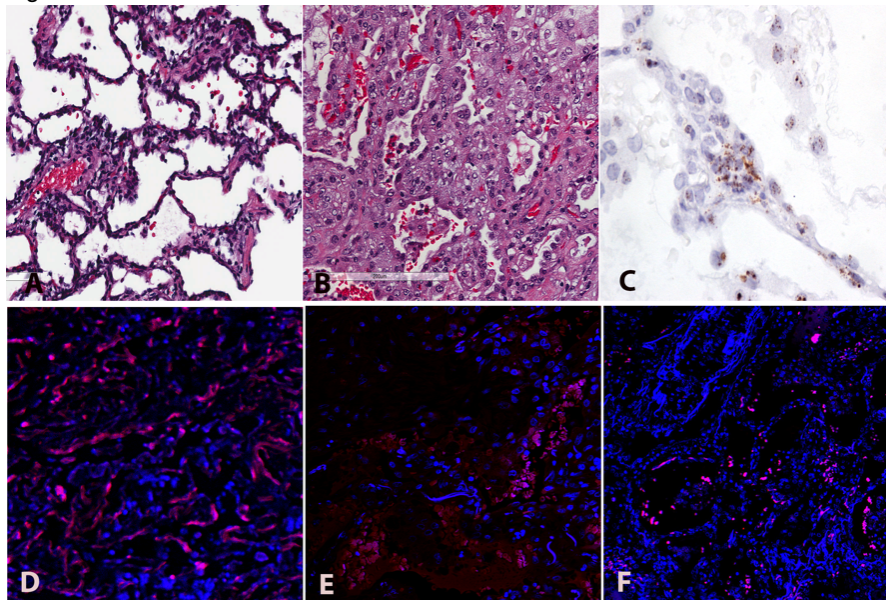


Figure 1. A. H&E of patient with 1 day interval, B. H&E of patient with 37 day interval, C. ISH for minus-strand viral RNA to detect replication, D. DIF for patient with 1 day interval, E. DIF for patient with 19 day interval, F. DIF for patient with 37 day interval

Conclusions: COVID-19 pneumonitis in this series of living patients was characterized by an interstitial mononuclear cell infiltrate which increased with time. This finding is in contrast to diffuse alveolar damage seen in patients who die in the acute phase of disease. The presence of ISH minus strand viral RNA and spike protein weeks after infection suggests that viral replication can persist for a long period.

767 Mucosal Eosinophilic Infiltration May be a Characteristic of Human Intestinal Spirochetosis

Sho Ogata¹, Ken Shimizu², Susumu Tominaga¹, Susumu Matsukuma¹

¹National Defense Medical College, Tokorozawa, Japan, ²JCHO Saitama Medical Center, Saitama, Japan

Disclosures: Sho Ogata: None; Ken Shimizu: None; Susumu Tominaga: None; Susumu Matsukuma: None

Background: Human intestinal spirochetosis (HIS) is a bacterial infectious disease of human large intestines, and most HIS cases are asymptomatic or exhibit mild intestinal symptoms. The host reaction to HIS remains unclear.

Design: We examined HIS-related mucosal inflammatory features histologically. From the archival HIS cases in a single medical center, 24 endoscopically taken specimens from 14 HIS cases (M:F = 10:4; 28-73 yrs) were selected as not containing polypoid or neoplastic lesions. Stromal and intraepithelial neutrophils and eosinophils, and stromal mast cells were counted, and the presence or absence of lymphoid follicles/aggregates was also examined. Association of the above inflammation parameters and spirochetal infection parameters (such as degrees of characteristic fringe distribution, of spirochetal cryptal invasion, and of spirochetal intraepithelial invasion) were also analysed.

Results: Intraepithelial neutrophils were observed in 29.2%, intraepithelial eosinophils in 58.3%, and lymphoid follicles in 50.0% of the specimens. Maximal stromal neutrophil, eosinophil, and mast cell counts averaged 8.4, 21.5, and 6.0, respectively, while intraepithelial neutrophils and eosinophils were 0.5 and 1.5, respectively. Strong correlation between iNeu and iEo ($p < 0.001$, $r = 0.81$), and correlations between iEo and sNeu ($p = 0.0012$, $r = 0.62$) and between iEo and sEo ($p = 0.026$, $r = 0.45$) were observed. Intraepithelial neutrophilic infiltration was influenced by fringe formation ($p < 0.05$) and spirochetal crypt involvement ($p < 0.05$).

Conclusions: HIS was accompanied by inflammatory reactions, including eosinophilia, lymphoid follicles/aggregates, and intraepithelial neutrophils and eosinophils. Among these, mucosal eosinophilic infiltration may be a central indicator and host reaction of HIS.

768 Galactomannan-Negative Aspergillus Fumigatus Presents with Unusual Morphology in Pediatric Patient with Septic Emboli and Complicated Medical History

Kara Roncin¹, Sree Sarah Cherian²

¹University Hospitals Cleveland Medical Center, Case Western Reserve University, Lyndhurst, OH, ²Case Western Reserve University/University Hospitals Cleveland Medical Center, Cleveland, OH

Disclosures: Kara Roncin: None; Sree Sarah Cherian: None

Background: Invasive aspergillosis caused by *Aspergillus fumigatus* has been well documented within the literature, with recent focus on molecular variations that have the potential to change pathogenicity of *A. fumigatus* when exposed to different environmental stressors. The majority of publications devoted to clinical cases of invasive aspergillosis focus on immunocompromised patients.

Design: Here we present the case of a 15-year old female without neutropenia or use of high dose corticosteroids, who presented with fevers, tachypnea, and numerous unprovoked septic thrombi following recent recovery from SARS-CoV-2 infection (COVID-19) without associated thrombotic complications.

Imaging revealed multiple large thrombi involving the right atria, right main pulmonary arteries, and hepatic veins. There was a suspected abscess within the lower lobe of the right lung in addition to diffuse peripheral and right basilar interstitial changes. Lymphadenopathy involving the mediastinum, right paratracheal, and subcarinal lymph nodes was present.

Results: Samples from right atrial thrombi and bronchial alveolar lavage were positive for septate hyphae on fluorescent staining. On solid agar, white, slow-growing fungal colonies appeared within one week of incubation (Figure 1). On microscopic examination with lactophenol cotton blue, the fungus demonstrated septate hyphae, absence of conidia, rare conidiophores with bare vesicles, and numerous structures consistent with terminal and intercalary chlamydospores (Figure 2). Matrix assisted laser desorption ionization-time of flight mass spectrometry (MALDI-TOF MS) performed on the fungal isolate was positive for *A. fumigatus*, which was confirmed via broad range PCR (utilizing a nested ITS primer set).

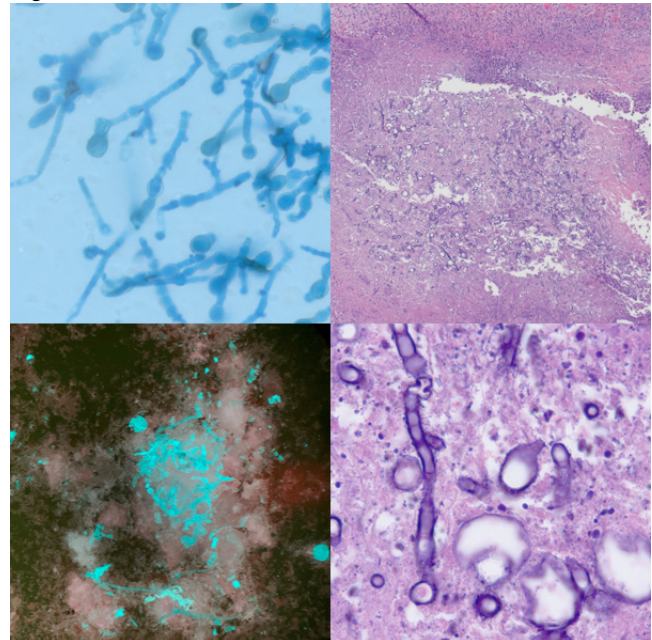
While Beta-D glucan was positive on serum, the galactomannan immunoenzymatic assay (EIA) was negative on both serum and CSF.

Fungal antibodies for *Aspergillus spp* and *Blastomyces spp* were negative, however, a second antibody assay for *Aspergillus spp* was positive.

Figure 1 - 768



Figure 2 - 768



Conclusions: In this patient galactomannan remained negative despite invasive aspergillus infection, and similar cases have been documented, thought to be related to low levels of circulating galactomannan below the limit of detection of the EIA test. The unusual microscopic appearance of the isolate with chlamyospore formation suggests a response to unfavorable conditions, due to which inadequate levels of galactomannan may have been released into the serum for conventional detection.

769 Atypical/Clonal T-lymphoid Populations in Splenic Parenchyma in Babesia Infection Associated with Splenic Rupture

Diana Treaba¹, Mikhail Gorbounov², Lee Cross³, Jennifer Mingrino², Fouad Zakka³, Stephanie Riviere², Cynthia Jackson⁴, Karren Ferreira³, Habibe Kurt⁵, Patrycja Dubielecka-Szczerba⁵, Evgeny Yakirevich⁴
¹Brown University Lifespan Academic Medical Center, Providence, RI, ²Brown University, Rhode Island Hospital, Providence, RI, ³Brown University, Rhode Island Hospital, Lifespan, Providence, RI, ⁴Rhode Island Hospital, Providence, RI, ⁵Alpert Medical School of Brown University, Providence, RI

Disclosures: Diana Treaba: None; Mikhail Gorbounov: None; Lee Cross: None; Fouad Zakka: None; Stephanie Riviere: None; Karren Ferreira: None; Habibe Kurt: None; Evgeny Yakirevich: None

Background: Discovered by the Romanian microbiologist Dr. Victor Babes in 1885, babesiosis is a worldwide spread zoonosis, endemic in the northeastern and upper midwestern USA regions. Transmitted by tick bite (*I. scapularis*), the clinical disease can range from asymptomatic, to a mild febrile illness, and in some patients to a severe or even fatal disease. The presentation of babesiosis with splenic rupture has a mechanism still incompletely understood.

Design: We describe three cases of patients infected with Babesia species who presented/developed splenic rupture. The men were 47 and 48 years old respectively, while the woman was 58 years old. Their degree of parasitemia at presentation was 0.11%, 0.42% and 0.37%. They all tested negative for Anaplasma (morphology and PCR) and the 48 year old man had a mildly elevated Lyme reflex (1.13; range 0-0.91), while the others tested negative. All patients presented with splenic rupture and underwent splenectomy. The spleen specimens were submitted for histopathological and immunophenotypical evaluation.

Results: All patients had anemia and thrombocytopenia at presentation (see Table 1). The spleens weighed 256, 382 and 299g. Histopathologic examination was notable for expanded white pulp containing parenchymal regions with recent hemorrhage, and an increased population of histiocytes in a small subset with hemophagocytosis. The

white pulp was preserved, had primary and secondary follicles, some with variable degree of apoptosis of their germinal centers. By immunohistochemistry, the red pulp had an increased CD3+, CD56-, CD30-, TdT- T-lymphoid population with partial loss of CD5 and bcl2, with a slightly reversed CD4 to CD8 cell ratio, and in the single case where flow cytometry was performed the CD4 to CD8 cell ratio was 0.6, and there was detected a subset (33% of the T-cells) of CD8+ T-lymphoid cells with partial loss of CD5, and also a subset (20%) of double negative (CD4 and CD8) T-lymphoid cells also with partial loss of CD5. The B-lymphoid cells were polytypic. Molecular studies were performed only in two cases, and detected only in one case minor T-cell receptor beta and gamma T-cell receptor gamma gene rearrangements. Of interest, two cases had also a few EBER positive nuclei suggestive of possible associated co-infection.

Age	Sex	Degree of parasitemia	Hgb g/dL	WBC x10 ⁹ /L	Plts x10 ⁹ /L	Spleen grams	PCR	EBER
47	M	0.11%	10.1	10.9	78	256	Minor clonal <i>TRB</i> and <i>TRG</i> rearrangements	Negative
48	M	0.42%	8.6	2.7	59	382	Negative for <i>TRB</i> , <i>TRG</i> and <i>IGH</i> rearrangements	A small loose aggregate of positive cells
58	F	0.37%	9.7	3.2	91	299	Not done	Rare positive cells

Conclusions: While atypical/clonal T-lymphoid populations have been reported in infectious processes, this is the first report identifying the presence of atypical/clonal T-lymphoid population(s) in splenic parenchyma of patients with Babesia infection with associated splenic rupture.

770 SARS-CoV-2 Related Biomarker Investigation: Lessons from a Single Institution Autopsy Series

Xiaoming (Mindy) Wang¹, Rahul Mannan², Yuanuan Qiao¹, Eman Abdulfatah², Allecia Wilson¹, Jeffrey Jentzen¹, Lisa McMurry³, Carol Farver⁴, Jeffrey Myers⁵, Liron Pantanowitz¹, Sylvia Zelenka-Wang³, Yuping Zhang³, Xuhong Cao¹, Arul Chinnaiyan¹, Rohit Mehra¹
¹University of Michigan, Ann Arbor, MI, ²Michigan Medicine, University of Michigan, Ann Arbor, MI, ³Michigan Center for Translational Pathology, Ann Arbor, MI, ⁴University of Michigan School of Medicine, Ann Arbor, MI, ⁵Michigan Medicine, Ann Arbor, MI

Disclosures: Xiaoming (Mindy) Wang: None; Rahul Mannan: None; Eman Abdulfatah: None; Jeffrey Jentzen: None; Lisa McMurry: None; Carol Farver: None; Jeffrey Myers: None; Liron Pantanowitz: None; Sylvia Zelenka-Wang: None; Yuping Zhang: None; Xuhong Cao: None; Arul Chinnaiyan: None; Rohit Mehra: None

Background: COVID-19 was declared a pandemic in March 2020 by the World Health Organization. As of 14 October 2020, more than 38.3 million cases have been confirmed, with more than 1.08 million deaths. COVID-19 affects multi-organ systems with the highest impact noted in the respiratory, cardiovascular, gastrointestinal, neurological, renal and immune organs in humans. COVID-19 is caused by severe acute respiratory syndrome coronavirus 2 (SARS-CoV-2), a positive-sense single-stranded RNA virus. This virus enters host cells through attachment of the viral spike (S) glycoproteins to the host transmembrane receptor protein, the angiotensin-converting enzyme 2 (ACE2), followed by spike protein cleavage and activation by cell surface transmembrane protease serine 2 (TMPRSS2). Knowledge about the spectrum of SARS-CoV-2 infection, ACE2 and TMPRSS2 expression in various human organs would benefit our understanding of the infection mechanism and potential future therapies.

Design: In this study, we performed pathology and biomarker characterization in 6 COVID-19 autopsy cases with interrogation of several organ systems affected by SARS-CoV-2. Specifically, we utilized an RNA *in situ* hybridization (RNA-ISH) approach to survey the localization of SARS-CoV-2 virus with a probe against the S gene (V-nCoV2019-S), virus replication with a probe against the anti-sense of the S gene (V-nCoV2019-S-sense),

host entry receptor ACE2, and priming protease TMPRSS2, in postmortem human tissues. The presence of SARS-CoV-2 virus was correlated with the expression of host entry machinery in the affected organs.

Results: V-nCoV2019-S stain was visualized as individual brown punctate dots or clusters. SARS-CoV-2 virus were detected in the respiratory tract (trachea, bronchus, lung parenchyma), colon, liver, thyroid, lymph node, kidney and prostate. Viral signals were not detected in heart, adrenal, pancreas, stomach, small intestine, or uterus in this cohort. By V-nCoV2019-S-sense probe RNA-ISH evaluation, we detected viral replication as brown signal clusters in all organ systems where virus was detected, except lymph node. Viral presence was heterogeneous among tissue sections sampled from different lobes of the lung and different areas of non-pulmonary tissues. The density of SARS-CoV-2 virus was variable among different organs and cases, with higher abundance in the respiratory tract. The highest virus abundance was observed in a patient who was immunocompromised secondary to renal transplant for end-stage diabetic nephropathy. ACE2 and TMPRSS2 were detected in all organ systems where virus was detected, except colon; ACE2 was also detected in the heart and uterus.

Table 1. Clinical characteristics of the 6 COVID-19 autopsy cases.

Case ID	Age	Gender	Race	Histopathology and final diagnosis	Other significant conditions
1	53	M	Caucasian	Diffuse alveolar damage, acute, exudative phase	Type A aortic dissection-operated
2	46	M	African American	Adult respiratory distress syndrome, proliferative diffuse alveolar damage, and acute renal failure	Cardiomegaly: myofibrillary hypertrophy; Hpatomegaly: mild to moderate steatosis; hypertension, diabetes and obesity
3	79	F	Caucasian	Adult respiratory distress syndrome	Ischemic bowel disease, hypotension: caridomegaly, myofibrillary hypertrophy, end stage kidneys status post-transplant
4	37	M	Caucasian	Diffuse alveolar damage, fibrinous pneumonia	Asthma, hemorrhage, edema and mucus plugging, hemopericardium, pleural effusions and ascites
5	80	M	African American	Diffuse alveolar damage, acute and organizing bronchopneumonia, hemorrhage and edema	Coronary artery disease, hypertension, type 2 diabetes mellitus
6	66	M	Caucasian	Under Review	Under Review

Conclusions: SARS-CoV-2 virus was detected in postmortem human respiratory tract, gastrointestinal, genitourinary, and immune systems where key components of the host’s cellular entry machinery, ACE2 and TMPRSS2, were concordantly expressed.